AIP | Applied Physics Letters

Cesium-doped zinc oxide as electron selective contact in inverted organic photovoltaics

Achilleas Savva and Stelios A. Choulis

Citation: Appl. Phys. Lett. **102**, 233301 (2013); doi: 10.1063/1.4811088
View online: http://dx.doi.org/10.1063/1.4811088
View Table of Contents: http://apl.aip.org/resource/1/APPLAB/v102/i23
Published by the AIP Publishing LLC.

Cesium-doped zinc oxide as electron selective contact in inverted organic photovoltaics

Achilleas Savva and Stelios A. Choulis[a)]
Molecular Electronics and Photonics Research Unit, Department of Mechanical Engineering and Materials Science and Engineering, Cyprus University of Technology, Limassol 3603, Cyprus

(Received 1 April 2013; accepted 22 May 2013; published online 11 June 2013)

Water based sol-gel processed Cesium-doped Zinc oxide (CZO) with low processing annealing temperature is introduced as an efficient electron selective contact in inverted Organic Photovoltaics (OPVs). The corresponding inverted OPVs not only demonstrate similar performance compared to the well-established sol-gel processed ZnO inverted devices but also maintain their functionality when thick layers of CZO, suitable for the up scaling scenario of OPVs have been used. The three orders of magnitude higher conductivity of CZO than ZnO in combination with the high transmittance above 80%, makes this doped oxide a suitable electron selective contact for the low-cost, roll-to-roll printing process of OPVs. © *2013 AIP Publishing LLC*. [http://dx.doi.org/10.1063/1.4811088]

Solution based organic photovoltaics (OPVs) are becoming an extremely active area of research, in order to meet the urgent need for clean and renewable sources of energy. Despite exhibiting lower power conversion efficiency (PCE) in comparison to conventional inorganic technologies, OPVs have attracted particular attention due to their flexibility, low weight, and compatibility with printing roll-to-roll (R2R) processes.[1] Inverted single and tandem OPVs in particular could allow more flexibility on designing the R2R production process and thus provide technological opportunities.[2,3] Despite the recent progress, further optimisation of electrodes carrier selectivity is an essential parameter for improving the performance of inverted OPVs.[4]

Efficient inverted OPVs[5,6] require highly transparent and conductive layers, which are inserted between the indium tin oxide (ITO) and the photoactive layer to provide appropriate electron carriers selectivity. The most common materials used for this purpose are n-type transition metal oxides, like TiOx (Ref. 7) and ZnO,[8] prepared by employing sol-gel processes[9] or colloidal nanoparticle dispersions in various solvents.[10] However, in many cases, solution processed metal oxides require the use of hazardous chemicals and high post-deposition temperature treatments[11] in order to achieve high electrical conductivity. The use of hazardous chemicals and the high temperature processing steps usually involved for solution processed metal oxides are parameters, which are not compatible with the environmental friendly and flexible OPV technology product development targets.

One way to overcome the above limitations is to dope metal oxides in order to enhance their electrical conductivity.[12] Doped metal oxides can allow the fabrication of relatively thick conductive layers without significant increase of the device internal resistances. Thicker and more conductive films that are produced with non-toxic solvents during processing are favorable for the up-scaling R2R printing scenario of OPVs.[2] Additionally, highly conductive doped metal oxides are widely used as intermediate layers of tandem OPVs as well as for transparent electrodes in organic optoelectronic devices.[13,14] Numerous ways of doping ZnO were suggested in the literature.[15–18] Recently, Krebs *et al.* introduced aluminum-doped zinc oxide (AZO) as an electron selective contact in OPVs produced by water based sol–gel method.[2] Stubhan *et al.* studied the effect of the AZO on inverted OPVs operation. They concluded that despite the use of non-toxic solvents and the thick high conductive layers used the postdeposition annealing treatment used has to be further reduced in order to meet their compatibility with flexible substrates.[12]

Cesium compounds have been previously investigated in OPVs and results have indicated that can serve as an efficient electron transporting layer in superstrate (normal)[19] and inverted OPV structures.[20–22] In this study, we present an approach of doping the ZnO with cesium, using water based sol-gel process. Although usually high temperature annealing is essential for enhanced functionality of the oxide layers, our proposed doped oxide importantly exhibits exceptional conductivity and transmittance values when annealed at lower temperature (140 °C for 25 min in air), a parameter that is critical for flexible OPVs processing requirements. Inverted OPVs using ITO/ZnO/Poly(3-hexylthiophene-2,5-diyl):Phenyl-C61-butyric acid methyl ester(P3HT:PCBM)/Poly(3,4-ethylenedioxythiophene):poly(styrenesulfonate)(PEDOT:PSS)/Ag are compared with those comprising ITO/cesium-doped zinc oxide (CZO)/P3HT:PCBM/PEDOT:PSS/Ag. We show that OPVs using thin ZnO and CZO as electron selective contacts exhibit similar device performance. However, thicker ZnO un-doped layers resulted to reduced PCEs due to fill factor (FF) and current density (Jsc) losses. The origin of the PCE loss is the increased series resistance (Rs) for the OPVs using thick un-doped ZnO as electron selective contact something which is proved by the current density against voltage characteristics and external quantum efficiency (EQE) measurements presented later within the text. In contrast, devices using thicker doped CZO electron selective contact illustrate comparable PCE with devices using thinner CZO buffer layers. The inverted OPVs investigated in this work as well as the simplified process flow for the solution based ZnO and CZO electrons selective contacts used are described in Fig. 1.

The ZnO precursor has been prepared using a zinc acetate dehydrate, monoethanolamine as a stabilizer dissolved

a)Electronic mail: stelios.choulis@cut.ac.cy

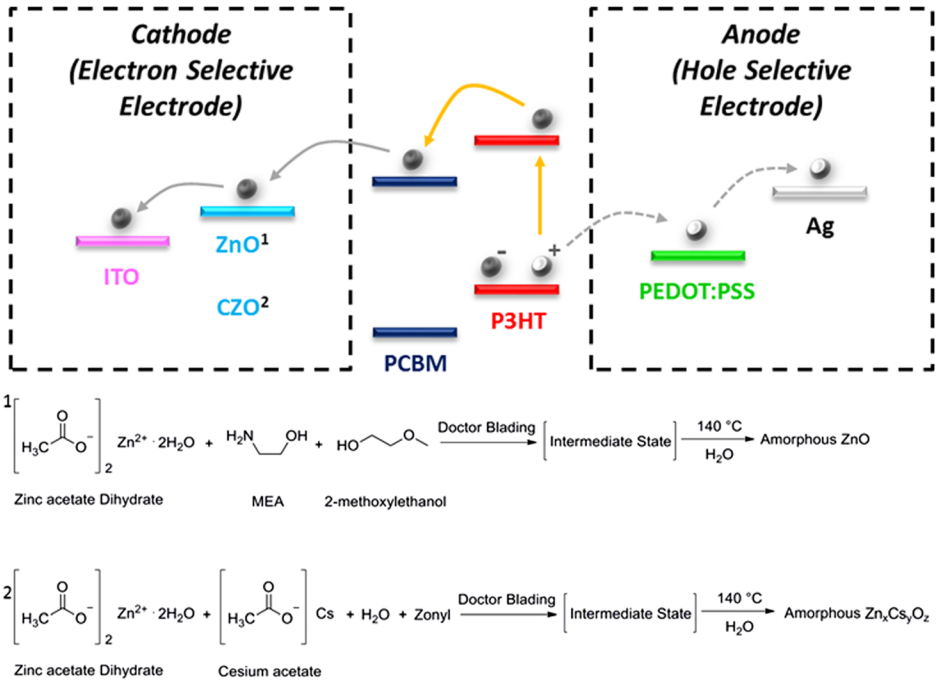

FIG. 1. Relative energy diagram of inverted OPVs under study depicting the basic steps for electron and hole collection, after the creation and separation process of the exciton within the active blend. In addition a simplified process flow for the solution based electron selective contacts used in this study, ZnO and CZO.

in 2-methoxyethanol. CZO films precursor solution has been fabricated using a water based sol-gel process. 0.5 g of zinc acetate dehydrate has been mixed with 0.005 g (1 mol. %) of cesium acetate dissolved in 5 ml of water and 0.015 g of zonyl FS-300. The solution has being stirred at 80 °C for 2 h and then filtered with 45 μm porous nylon filters. The resulting precursor can be kept in ambient conditions and used efficiently in devices for several months. Both of the precursor solutions have been printed using doctor blading on top of ITO substrates and annealed after deposition, at 140 °C for 25 min in air. P3HT:PCBM solutions (1:0.8 in cholorobenzene) have been doctor bladed on top of the oxide layers resulting in a layer thickness of 230 nm. The device top electrode has been fabricated according to our previously published data using PEDOT:PSS with additives and an evaporated 100 nm silver (Ag) top contact.[23]

In order to investigate the effect of doping the ZnO with cesium on the electronic and surface properties of the resulting CZO, a series of measurements have been performed such as electrical conductivity, transmittance, contact angle, and atomic force microscopy (AFM) measurements. Electrical conductivity has been measured by applying the four point probe technique[24] and using a Jandel RM3000 unit, equipped with a linear array, tungsten carbide four point probe head. Because of the low conductivity of these semiconducting materials, relatively thick layers are required in order to be able to measure their sheet resistance. For this purpose, CZO and ZnO (4 μm thick) have been fabricated under similar processing condition used for the processing of the functional electron selective contacts used for the inverted OPVs device fabrication. To fabricate the thicker films of the oxides, the doctor-bladed speed was modified while all the other processing and precursor solution parameters kept constant. When 10 nA of current was passing between the probes, doped ZnO oxide (CZO) exhibited three orders of magnitude lower sheet resistance (9 kOhm/sq) than the pristine ZnO (400 MOhm/sq). This results to 3 order of magnitude lower resistivity for the CZO (380 Ohm cm) than the un-doped ZnO (160 kOhm cm) and thus 3 orders of magnitude increased conductivity (2.77×10^{-3} S/cm) for CZO compared to the ZnO (6.25×10^{-6} S/cm).

Transmittance measurements have been performed using a schimadzu 2700 UV-Vis spectrophotometer. All the compared layers have been fabricated identically as the layers used for the inverted OPVs under study. 40 nm and 200 nm ZnO as well as 45 nm and 200 nm CZO have been subjected to transmittance measurements between 300 and 800 nm wavelengths. The results proved that the transmittance is independent of the layer thickness since both oxides (ZnO and CZO) exhibit transmittance above 80% for all the visible spectrum between 400 nm and 800 nm, and absorption occurs only in wavelengths below 400 nm.

Contact angle measurements[25] have been performed using KRUSS DSA 100E goniometer on the surface of the same films used for the transmittance measurements. The water contact angle has been found to be slightly reduced on the surface of the two CZO (57°) layers compared to ZnO (73°). This is a possible indication that CZO is slightly more hydrophilic than ZnO. Although water contact angle on the surface of CZO is reduced compared to the contact angle deposited on the surface of ZnO, P3HT:PCBM contact angle, which is the upper-layer in inverted OPVs under study, exhibits the same contact angle on top of both of the compared electron selective contacts and thus it is unlikely that the potential hydrophilicity difference of the two metal oxides layers under study to alter the active layer (AL) (P3HT:PCBM) morphology.

Finally, in order to examine the surface topography of the two compared electron selective contacts, AFM studies were performed. Using a Nanosurf equipment, tapping mode AFM was applied on the surface of 200 nm thick ZnO and CZO which were fabricated identically with the layers used for the inverted OPVs under study.

The measurements compare the surface topography of sol-gel derived ZnO (Fig. 2(a)) with the cesium doped oxide used in this study CZO (Fig. 2(b)). The two layers exhibit

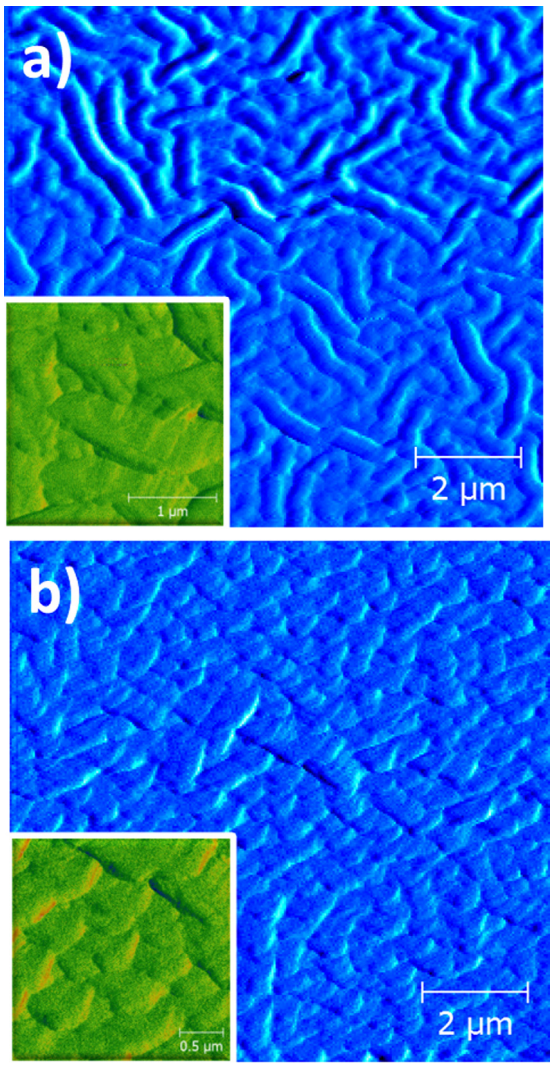

FIG. 2. Tapping mode $10 \times 10\,\mu$m atomic force microscopy images for (a) sol-gel derived ZnO and (b) sol-gel derived CZO. The insets represent tapping mode $2.5 \times 2.5\,\mu$m for each corresponding measurement.

altered surface topography, showing different aggregation between the two compared films. ZnO exhibits larger and differently oriented aggregates than CZO. On the other hand, CZO AFM image demonstrates more ordered surface aggregation. The surface roughness of CZO was found to be 1.13 nm compared to 7.2 nm for the ZnO film. The relatively smoother surface of CZO is a possible reason for the reduce contact angle of water on top of its surface compared to the water contact angle on top of ZnO. Table I summarizes the critical measurement values performed for ZnO and CZO electron selective contacts.

Subsequent to functional ZnO and CZO metal oxides layers characterization, inverted OPVs using ZnO and CZO electron selective contacts between the transparent electrode and the P3HT:PCBM AL were fabricated. The inverted OPVs top electrode was kept identical for all devices under study (PEDOT:PSS:Additive/Silver) and has been fabricated as described previously in the text.[24] Four series of devices have been compared to investigate the effect of metal oxide doping on inverted OPV performance. The selected inverted OPV device structures under study described as follows: (1) ITO/ZnO(40 nm)/AL/top electrode, (2) ITO/ZnO(200 nm)/AL/top electrode, (3) ITO/CZO(45 nm)/AL/top electrode, and (4) ITO/CZO(200 nm)/AL/top electrode. To adjust the thickness of the compared metal oxide based (CZO and ZnO) electron selective contacts, the doctor-blading speed was varying while all the other processing parameters such us temperature, blade height and precursor's volume and concentration have been kept constant. The four metal oxide electron selective contacts under comparison have been annealed for 25 min at 140 °C in air, prior to deposition of the following layers of the inverted OPVs.

Fig. 3, upper plot (3(a)) demonstrates the inverted OPVs current density against voltage characteristics (J/V) and the EQE of the inverted OPVs under study. The J/V characteristics were measured with a Keithley source measurement unit (SMU 2420). For illumination a calibrated Newport Solar simulator equipped with a Xe lamp was used, providing an AM1.5G spectrum at 100 mW/cm^2. EQE measurements were carried out on a Newport setup comprising a Xe lamp, a monochromator, a current-voltage preamplifier, and a lock-in amplifier.

The devices using the synthesized CZO (45 nm) as electron selective contact exhibit similar PCE as the inverted devices using the well-established sol-gel processed ZnO. The PCE performance parameters for the compared devices show similar values of Open-circuit Voltage (Voc) 0.59 and 0.58 V, current density (Jsc) 9.0 and 8.9 mA/cm^2 as well as FF values of 66% and 63%, resulting to PCE of 3.46% and 3.28%, respectively. In addition, the devices using 200 nm of CZO illustrate comparable device performance Voc-0.57 V, Jsc-8.71 mA/cm^2, FF-62%, PCE-3.07%, with the devices using 45 nm of CZO as electron selective contact. On the other hand, when the thickness of the ZnO is increased to 200 nm the performance parameters are significantly reduced, Voc-0.55 V, Jsc-6.05 mA/cm^2, FF-55%, PCE-1.86%, compared to the control devices using 40 nm ZnO.

The above observations can be explained by the inset of Fig. 3(a) which demonstrates the series resistance (Rs) regime of the dark J/V characteristics for the inverted OPVs under study. The devices using 40 nm ZnO demonstrate comparable Rs with the device using 45 nm CZO as electron selective contact and thus similar device performance. Furthermore, the

TABLE I. Synopsis of the major optoelectronic and surface properties values for the metal oxides used in this study.

Layer	Conductivity [S/cm]	Transmittance at 400–800 nm [%]	Water contact angle [°]	P3HT:PCBM contact angle [°]	Surface roughness [nm]
40 nm ZnO	…	>80	71	23	…
45 nm CZO	…	>80	58	22	…
200 nm ZnO	6.25×10^{-6}	>80	73	22	7.2
200 nm CZO	2.77×10^{-3}	>80	57	20	1.13

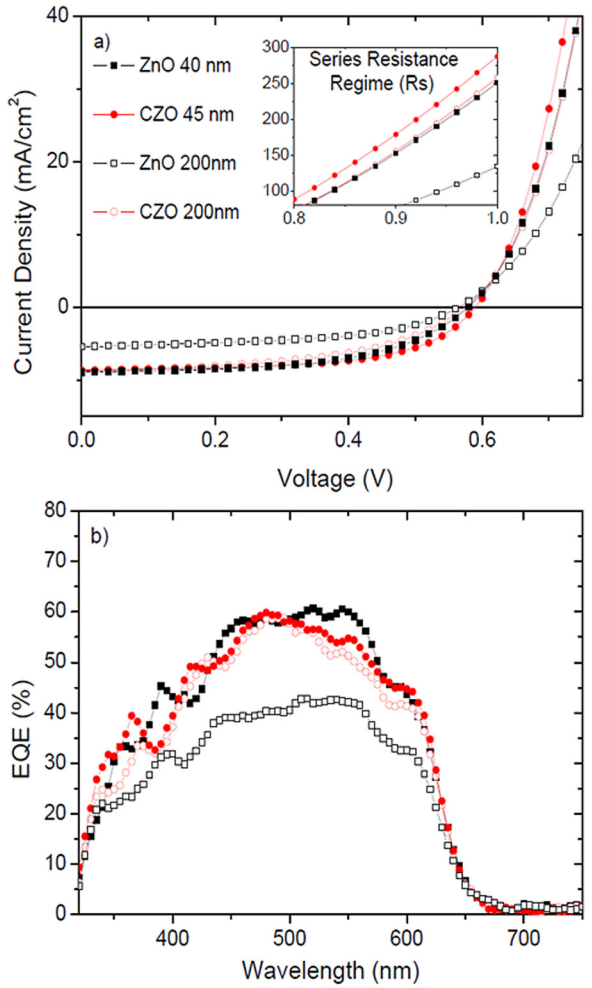

FIG. 3. Illuminated J/V characteristics of inverted OPVs under study. The inset of Fig. 3(a) demonstrates the series resistance (Rs) regime of the dark J/V characteristics for the inverted OPVs under study. (b) External quantum efficiency for the same inverted OPVs used in Fig. 3(a) by the inset.

devices using 200 nm CZO exhibit similar Rs when compared with the inverted OPVs using thin ZNO and CZO as electron selective contact. In contrast, the Rs of the inverted OPVs using 200 nm ZnO is significantly increased compared with the other three inverted OPVs. The increased Rs is the origin of the Jsc and FF drop of the corresponding device compared to the other three inverted OPVs taking in mind that the transmittance and the wetting properties of the front electrode remain the same after ZnO thickness increase (see Table I). This pronounced difference in Rs between the two devices using thick electron transporting contacts arises from the difference in conductivity between the two compared materials as demonstrated previously within the text. As reported in the literature, the increased conductivity of the electrodes can affect the device OPVs performance by reducing the device internal resistances.[26] The values of the series resistance for all the diodes under study have been calculated using a simulation model described previously by Waldauf *et al.*[27]

In agreement with our previous observations, Fig. 3(b) demonstrates a significant reduction in the EQE percentage for the device using 200 nm ZnO as the electron selective contact compared to the other three inverted OPVs. Since the transmittance of the front electrode, active layer absorption properties, and hole selective contact (top electrode) are the same for all the inverted OPVs under comparison, the reduced EQE, for the thick un-doped ZnO, indicates a significant electron charge carrier losses within the device. The increased conductivity of the cesium doped oxide allows electron charges to be transferred and collected by the ITO without any significant losses even when thicker layers are used. In contrast, inverted OPVs with thick ZnO layers show significantly carrier losses during the collection process due to their conductivity limitations (Table II).

TABLE II. Photovoltaic parameters of the inverted OPVs under study, using different thickness ZnO and CZO as electron selective layers.

Device	Voc [V]	Jsc [mA/cm^2]	FF [%]	PCE [%]	Rs [Ohm]
40 nm ZnO	0.58	8.9	63	3.28	1.3
45 nm CZO	0.59	9	66	3.46	1.1
200 nm ZnO	0.55	6.05	62	1.86	3.8
200 nm CZO	0.57	8.71	62	3.07	1.5

The up scaling low-cost roll-to-roll printing scenario of OPV production demands thicker and efficient electron selective contacts, using non-toxic solvents for "clean" solution processed energy harvesting and low temperature annealing, suitable for flexible OPV technology. In the presented study we demonstrated a doped oxide, developed by water based sol-gel process, as an efficient electron selective contact in inverted OPVs. The low annealing temperature suitable to flexible OPV technology in combination with the exceptional inverted OPV performance when thick layers of CZO are utilized indicates the potential of the proposed doped oxide for the up scaling scenario of OPVs. The three orders of magnitude increased conductivity of CZO compared to the well-established sol-gel processed ZnO in combination with exceptional transmittance, surface and wetting properties makes this doped oxide a suitable candidate for use in a broad range of solution based organic and inorganic electronic applications.

We would like to thank Cyprus Research Promotion Foundation for funding the development of the Molecular Electronics and Photonics Research Unit at Cyprus University of Technology under Research Grant "NEA ΥΠΟΔΟΜΗ/ΣΤΡΑΤΗ/0308/06."

[1]F. C. Krebs, Sol. Energy Mater. Sol. Cells **93**, 394 (2009).
[2]R. Søndergaard, M. Helgesen, M. Jørgensen, and F. C. Krebs, Adv. Energy Mater. **1**, 68 (2011).
[3]M. M. Voigt, R. C. I. Mackenzie, C. P. Yau, P. Atienzar, J. Dane, P. E. Keivanidis, D. D. C. Bradley, and J. Nelson, Sol. Energy Mater Sol. Cells **95**, 731 (2011).
[4]D. J. D. Moet, P. de Bruyn, and P. W. M. Blom, Appl. Phys. Lett. **96**, 153504 (2010).
[5]C. Waldauf, M. Morana, P. Denk, P. Schilinsky, K. Coakley, S. A. Choulis, and C. J. Brabec, Appl. Phys. Lett. **89**, 233517 (2006).
[6]A. Savva, F. Petraki, P. Elefteriou, L. Sygellou, M. Voigt, M. Giannouli, S. Kennou, J. Nelson, D. D. C. Bradley, C. J. Brabec, and S. A. Choulis, Adv. Energy Mater. **3**, 391 (2013).
[7]R. Steim, S. A. Choulis, P. Schilinsky, and C. J. Brabec, Appl. Phys. Lett. **92**, 093303 (2008).
[8]A. Manor, E. A. Katz, T. Tromholt, and F. C. Krebs, Sol. Energy Mater. Sol. Cells **98**, 491 (2012).
[9]T. Kuwabara, C. Tamai, Y. Omura, T. Yamaguchi, T. Taima, and K. Takahashi, Org. Electron. **14**, 649 (2013).

[10]H. Oh, J. Krantz, I. Litzon, T. Stubhan, L. Pinna, and C. J. Brabec, Sol. Energy Mater. Sol. Cells **95**, 2194 (2011).
[11]M. S. White, D. C. Olson, S. E. Shaheen, N. Kopidakis, and D. S. Ginley, Appl. Phys. Lett. **89**, 143517 (2006).
[12]T. Stubhan, H. Oh, L. Pinna, J. Krantz, I. Litzov, and C. J. Brabec, Org. Electron. **12**, 1539 (2011).
[13]N. Li, T. Stubhan, D. Baran, J. Min, H. Wang, T. Ameri, and C. J. Brabec, Adv. Energy Mater. **3**, 301 (2013).
[14]J. Owen, M. S. Son, K.-H. Yoo, B. D. Ahn, and S. Y. Lee, Appl. Phys. Lett. **90**, 033512 (2007).
[15]T. Z. Oo, R. D. Chandra, N. Yantara, R. R. Prabhakar, L. H. Wong, N. Mathews, and S. G. Mhaisalkar, Org. Electron. **13**, 870 (2012).
[16]S. Ray, R. Das, and A. K. Barua, Sol. Energy Mater. Sol. Cells **74**, 387 (2002).
[17]M. J. Alam and D. C. Cameron, J. Vac. Sci. Technol. A **19**, 1642 (2001).
[18]A. Aprilia, P. Wulandari, V. Suendo, Herman, R. Hidayat, A. Fujii, and M. Ozaki, Sol. Energy Mater. Sol. Cells **111**, 181 (2013).
[19]M.-H. Park, J.-H. Li, A. Kumar, G. Li, and Y. Yang, Adv. Funct. Mater. **19**, 1241 (2009).
[20]H.-H. Liao, L.-M. Chen, Z. Xu, G. Li, and Y. Yang, Appl. Phys. Lett. **92**, 173303 (2008).
[21]G. Cheng, W.-Y. Tong, K.-H. Low, and C.-M. Che, Sol. Energy Mater. Sol. Cells **103**, 164 (2012).
[22]T. Xiao, W. Cui, M. Cai, W. Leung, J. W. Anderegg, J. Shinar, and R. Shinar, Org. Electron. **14**, 267 (2013).
[23]A. Savva, M. Neophytou, C. Koutsides, K. Kalli, and S. A. Choulis, "Synergetic effects of buffer layers processing additives to enhanced hole carrier selectivity in inverted organic photovoltaics," Org. Electron. (submitted).
[24]H. Wieber, *Laboratory Notes on Electrical and Galvanometric Measurements* (Elsevier, Amsterdam, 1979), p. 6.
[25]D. Y. Kwok and A. W. Neumann, Adv. Colloid Interface Sci. **81**, 167 (1999).
[26]P. Schilinsky and C. Waldauf, J. Appl. Phys. **95**, 2816 (2004).
[27]C. Waldauf, P. Schilinsky, J. Hauch, and C. J. Brabec, Thin Solid Films **451–452**, 503 (2004).